Journal of Materials Chemistry C

Swift Synthesis, Functionalization and Phase-transfer Studies of Ultrastable, Visible Light Emitting Oleate@ZnO Quantum Dots

Journal:	*Journal of Materials Chemistry C*
Manuscript ID	TC-ART-10-2015-003377
Article Type:	Paper
Date Submitted by the Author:	17-Oct-2015
Complete List of Authors:	Arslan, Osman; Bilkent University, Belkoura, Lhoussaine; University of Cologne, Department of Physical Chemistry Mathur, Sanjay; Institute of Inorganic Chemistry, University of Cologne, Chemistry Department

Journal of Materials Chemistry-C RSCPublishing

ARTICLE

Swift Synthesis, Functionalization and Phase-transfer Studies of Ultrastable, Visible Light Emitting Oleate@ZnO Quantum Dots

Cite this: DOI: 10.1039/x0xx00000x

Received ooth January 2012,
Accepted ooth January 2012

DOI: 10.1039/x0xx00000x

www.rsc.org/

Arslan O.[a] , Belkoura L.[b] and Mathur S.[a]*

Stable oleate capped, visible light emitting ZnO quantum dots (QDs) have been synthesized by a modified sol-gel method and examined for fabrication of large-scale synthesis. Surface chelation with oleate ligands and their implications on particle growth were investigated by comprehensive NMR experiments and photoluminescence measurements. High-resolution electron microscopy and X-ray diffraction confirmed the high crystallinity and well-dispersed character of ZnO QDs. Here investigated ZnO nanocrystals were found to be suitable for phase transfer synthesis (non-polar to polar dispersion medium) even after prolonged storage times that was verified by unchanged visible light emission. The absorption wavelength could be tuned by adjusting the nucleation kinetics and upon anchoring bulky ligands that provided control over surface defects responsible for optical (visible) properties. The demonstrated phase transfer studies make visible light emitting ZnO QDs accessible for a wide range of applications like ink-jet printing for nano-electronics, cell labelling or theranostic studies.

1 Introduction

Visible emission in ZnO nanostructures and its defect- and size-dependent photoluminescence properties have triggered great spurt of activities in the last years.[1-2] Metal chalcogenide quantum dots (CdSe, CdS, CdTe. etc.) have been the subject of more intense investigations due to their high quantum yields and controllable emission properties manifesting distinct size-property relationship. As a wide-band semiconductor, ZnO, has limited suitability for visible light absorption and emission, however its ready availability and functional implications in various fields such as transparent conductive oxides, light asborbers and photocatalysts has sustained the interest in its synthesis and modification.[3-5] Controlled generation of surface defects in ZnO nanocrystals and their modulation by organic surface chelators has been demonstrated to endow broadband emission throughout most of the solar spectrum. By varying the surface configuration, for instance, by tuning the oxygen vacancy control through ligand attachment and by creating interstitial defects (oxygen vacancies (V_o), oxygen interstitials (O_i), zinc vacancies (V_{zn}) and zinc interstitials (Zn_i), it is possible to tune the emission properties of the ZnO nanoparticles. Radiative recombination of the conduction band electron/valence band hole and its direct association with the UV absorption points out that UV absorption in ZnO nanocrystals exhibits confinement effect.[6-10] ZnO quantum dots synthesized by the sol-gel method tend to aggregate and ripen in the solution already at ambient conditions evident as a gradual red-shift in the fluorescence spectra.[11-16]

Liquid-phase synthesis of ZnO nanostructures starting from Zn-salt precursors has been widely studied, which typically involves dissolution of the Zn-salt followed by subsequent addition of alcohol and a strong base (NH_4OH, NaOH, KOH, LiOH) to precipitate out zinc hydroxide complex. The results show that base: metal precursor ratio is a critical and deterministic parameter the size and morphology of resulting ZnO nanostructures, for instance, high concentration of hydroxyl ions promotes the formation of tetra-hydroxo zincate complex that in turn leads to spontaneous nucleation with very high number of nuclei that decreases the overall particle size.[17] In alcoholic solutions, cations are shown to form a passivating layer providing a controlled growth and anti-agglomeration effect.[17] Therefore, by varying the counter ion, the size,

morphology and agglomeration can be altered.[18] Previous reports show that alcoholic conditions with LiOH as the base are favorable for metal doping.[18c]

Herein we report a facile method for the synthesis of ultrastable ZnO QDs by thermal decomposition of $Zn(Oleate)_2$ to tune the visible light emission by adjusting the experimental parameters and by varying the LiOH:Zn. Most salient impact of this work relates to the possibility of scaling-up the synthesis with selective luminescence properties along with their ultra-long stability of the Oleate@ZnO QDs. The results demonstrate that the presence of oleate ligands in the precursor molecule has a strong influence on the ZnO nucleation and growth phase as confirmed by NMR studies.

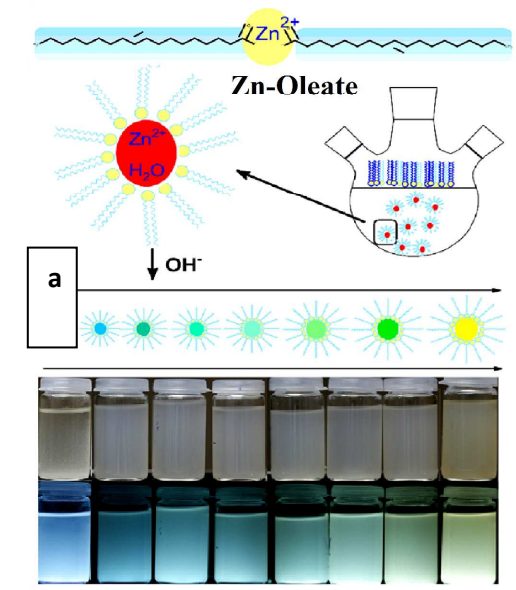

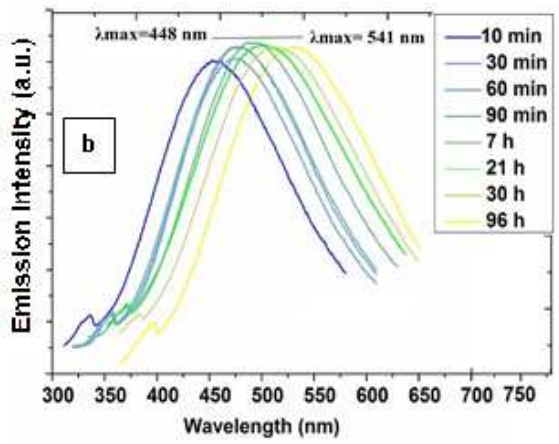

Figure 1: a) Synthesis of Oleate@ZnO QD's b) PL evolution of the Oleate@ZnO QD's

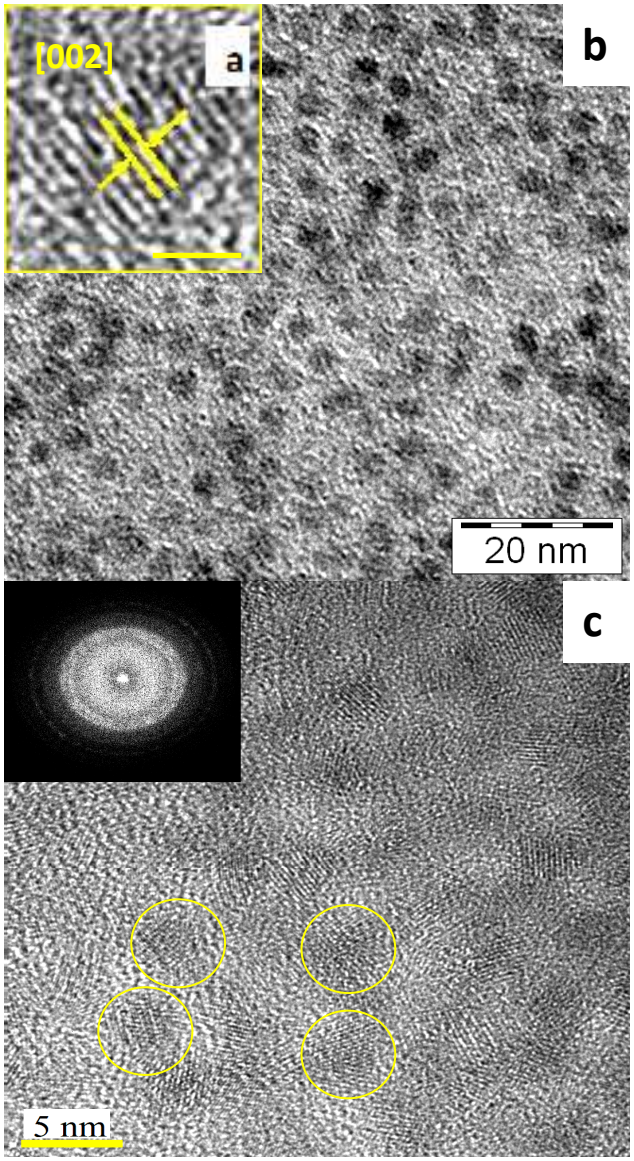

Figure 2: a)[002] spacing (0,26 nm) of Oleate@ZnO QD's (inset bar =2nm) b) TEM illustration of the Oleate@ZnO QD's c) HR-TEM images of Oleate@ZnO QD's (Inset is SAED pattern)

2 Experimental Details ZnO QDs (ZnO 1) were prepared by decomposition of $Zn(Oleate)_2$ (5 equiv.) in 150 ml of the EtOH/MeOH mixture (50:50, v/v) and $LiOH.H_2O$ (7 equiv.) under vigorous stirring at 80°C. The resulting milky solution was refluxed for 96 hours at the same temperature and under nitrogen atmosphere to obtain suspensions of ZnO QDs. Aliquots were collected at different time intervals (10, 30, 60, 90 minutes and 7, 21, 30, 96 hours) to investigate the photoluminescence behavior and to record the particle size evolution by optical absorption spectra. Similar synthesis procedure was applied for the swift synthesis of blue and green emitting ZnO QDs whereby the synthesis at 55 °C with Zn:LiOH ratio of 5:7 resulted with a very bright blue emission (ZnO-2) and with Zn:LiOH ratio of 1:2 showed green emission

(ZnO-3) under similar conditions. In an alternative synthesis, ZnO QDs (ZnO-4) were obtained using $Zn(OAc)_2.2H_2O$ as the zinc precursor and with Zn:LiOH ratio of 5:7 in a reaction mixture refluxed at 55 °C followed by the analysis of the aliquots after 10, 30, 60 and 90 minutes. The as-prepared ZnO QDs were precipitated out by adding hexane to the reaction mixture and subsequently washed with water, ethanol and acetone and dried in vacuum for 6h at 90 °C.

2.1 Phase Transfer Oleate-capped ZnO QDs were dispersed by ultrasonication (5 min.) in $CHCl_3$ till a clear solution was obtained. At higher particle concentrations, the solutions had slightly turbid appearances due to interparticle interactions and possible agglomeration. In a following step, gluconic acid, as aqueous phase soluble ligand, was added to the ZnO QDs suspension and ultrasonicated for 5 minutes, which was sufficient for the completion of the phase-transfer reaction. The reaction mixture was refluxed at 80 °C for 12 h, and filtered to obtain a solution of modified particles, which were washed with EtOH and acetone to obtain water-dispersible ZnO QDs.

2.2. Characterization Particle size and distribution in ZnO QDs were investigated on a TEM (LEO 912 Omega, Zeiss, Oberkochen, Germany) operated at 120kV with zero loss conditions. The energy-filtered electron micrographs were recorded with a high-speed scanning camera (sharp: eye, 2048 x 2048 pixels, TRS, Moorenweis, Germany) under remote control using the image acquisition system (iTEM, Olympus Soft Imaging Solutions GmbH, Münster, Germany) and carbon coated Cu grids. NMR spectras were recorded with a Bruker AVANCE II 300 spectrometer at 298 K; NMR spectroscopic frequencies (external standards):1H: 300.1 MHz (TMS) for detection of the ZnO QDs surface modification characteristics. The powder X-ray diffraction (XRD) patterns of as-synthesized and thermally treated ZnO QDs were measured with a STOE-STADI MP vertical system in transmission mode using Cu Kα (α=0.15406 nm) radiation. FT-IR (Fourier Transform Infrared) analyses have been carried out with Perkin Elmer-Spectrum 400 with Universal ATR Sampling Accessory in the 400-4000 cm^{-1} range. UV-Visible and photoluminescence measurements were carried out using Perkin-Elmer Lambda 950 and Yvon-Horiba FluoroMax-3, respectively. Confocal images for the HEK cells labeled with Gluconate@ZnO QDs were taken with confocal microscope (Leica, LSM TCS SP5). Thermal analysis and surface modification of the prepared ZnO QDs was carried out in the temperature range from 30 to 800 °C with a heating rate of 10°C/min under nitrogen atmosphere (flow rate; 25 ml/min) using Mettler Toledo TGA/DSC 1 Stare systems. Surface morphology of the QD layer and EDX analysis were acquired by Nova Nano SEM 430 on silicon substrates, which were ultrasonically cleaned in an acetone bath before use.

3. Results and discussion

In a typical synthesis, oleate-capped ZnO nanoparticles were grown by decomposition of a molecular precursor $Zn(Oleate)_2$[15] in EtOH at 80 °C to which stoichiometric amount of LiOH/MeOH mixture was added that caused an immediate change in the appearance of the reaction mixture (clear to milky). The resulting mixture was refluxed for 96 h under nitrogen atmosphere, during which the particle formation was regularly monitored by optical spectrum. Aliquots were slowly removed during the reflux procedure and n-hexane was added to the concentrated reaction mixture to precipitate the quantum dots termed as ZnO-1 in this work. Quantum dots were removed from the solution by centrifugation (10.000 rpm, 15 min.) and washed with water and acetone several times and dried at 95°C under vacuum for 24 h. It is widely known that generally high temperatures result in faster growth of metal oxide particles due to thermodynamic-push and as a result it is difficult to control the particle size-distribution.

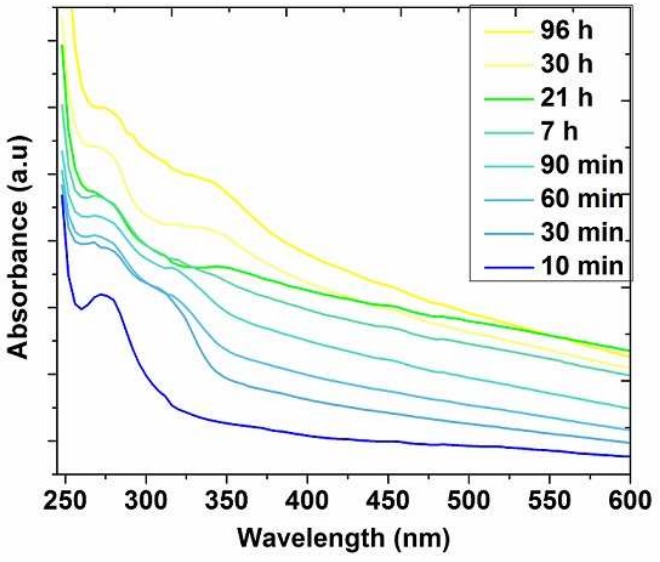

Figure 3: Evolution of the Oleate@ZnO QDs (ZnO-1)

Table 1: Size and optical properties of the oleate@ZnO-1 QDs

Synthesis Time	Size(a) (nm)	Size(b) (nm)	Band Gap(c) (eV)	Visible Maxima (eV)	UV Maxima (eV)
10 min	---	---		2,76	3,72
30 min	2,08	2,5	3,60	2,63	3,56
60 min	2,20	2,7	3,58	2,62	3,51
90 min	2,20	2,7	3,58	2,62	3,51
7 h	2,33	2,9	3,41	2,46	3,35
21 h	3,08	3,8	3,34	2,40	3,17
30 h	3,19	3,9	3,22	2,35	3,14
96 h	3,30	4,1	3,01	2,29	3,08

a) Obtained from UV-Vis absorption b) Obtained from effective mass model (me = 0.26 m_o, m_h = 0.59m_o, m_o is the,free electron mass, and Eg_{bulk} = 3.3 eV) c)From UV-Vis absorption

In this study, when the reflux time was limited to 90 minutes and temperature was lowered to 55 °C sharp and intense luminescence was observed from ZnO QDs by varying the Zn:LiOH ratio. At 55 °C, the Zn:LiOH ratio of 5:7 resulted in ZnO QDs (ZnO-2) with bright blue emission at λ_{max}, 442 nm. Switching the Zn: LiOH ratio to 1:2 with the similar reaction conditions produced ZnO QDs exhibiting a green-cyan visible emission (λ_{max}, 502 nm) (ZnO-3). For comparison sake, acetate modified ZnO QDs (ZnO-4) were synthesized from $Zn(OAc)_2.H_2O$ at 55 °C using a Zn: LiOH ratio of 5:7 that showed a remarkable shift from green (λ_{max}, 532) to orange (λ_{max}, 600 nm) in its colour and emission wavelength upon storage apparently due to weak coordination of acetate ligands on the surface of nanoparticles, which allows diffusion-driven growth in solution (Supporting Figure 2). When Zn/LiOH ratio is decreased growth of the QD formation has been accelerated and size of the QD's were bigger in magnitude detected via red shifted emission of the QD's.

NMR analysis and TEM images (Figure 4 and Supporting Figure 1) confirmed a core(ZnO)-shell(Oleate) structure with estimated shell thickness being ca. 3.5-4 nm. The FT-IR spectra showed only two main peaks at 1552 and 1402 cm^{-1} corresponding to the ligand backbone. TEM images of ZnO-1 with selective area electron diffraction (SAED) pattern (Figure 2) revealed a regular size-distribution with ZnO present in the wurtzite structure (verified by measuring d-d spacing of [002] facets as 0.26 nm). The crystal features of ZnO-2, ZnO-3 and ZnO-4 were found to be similar and were corroborated by measuring the lattice fringes (Figure 6). The evolution of optical absorption properties of the QDs during 96 h period (Figure 3) showed a gradual shift towards higher wavelength corresponding to particle growth that was supported by particle sizes and band gap energies calculated by employing the Meulenkamp equation[15] (Table 1). As seen in Figure 3, the initial 30 min of the reaction represents a transient regime with no clear impact of LiOH/MeOH mixture addition. This irregularity was always observed at every Zn:LiOH ratio and any applied temperature. The emission spectra of the Oleate@ZnO QDs revealed a stable nature of the quantum dots obtained after 90 minutes of refluxing. Based on this observation, highly stable Oleate@ZnO QDs with pronounced blue and green visible light emission were synthesized in relatively large amounts (3 g Oleate@ZnO QD) with potential for further scale up. The regular size of the as-synthesized ZnO QDs is also manifested in the high packing density of particles, when applied as suspensions on glass slides to form thin films. The intensity of blue emission in ZnO-2 (442 nm) was evidently higher (ca. 10 times) than the emission intensity of acetate-coated ZnO-4 (537 nm) as supported by their UV-Visible and PL measurements (Supporting Figure 2). It is known that UV emission arises from the band gap feature of the nanoparticle but visible emission can originate from different sources. TEM investigation shows that ZnO-4 is heavily agglomerated and the inter-particle contacts is pronounced that can be detrimental for the emission properties (physical quenching), while ZnO-1 is regularly distributed without observable aggregation (Supporting Figure 3).

1H NMR investigation of the Oleate@ZnO QDs supported the FT-IR spectra (Figure 8c and Supporting Figure 4). The NMR spectrum (Figure 4) of the capping ligand oleic acid exhibited chemical shifts at 5.36 ppm due to double bond protons (CH=CH) and the reference signal at 7.29 ppm due to $CDCl_3$. Methylene unit ($-CH_2$) present adjacent to the carbonyl group could be unambiguously assigned at 2.18 ppm. Additional peaks observed between 1.8-0.7 ppm are due to the remaining protons. Upon deprotonating, oleic acid forms an oleate ligand,

which significantly changes the NMR pattern. The NMR spectrum of the molecular precursor $Zn(oleate)_2$ showed that resonance peak of the double bond protons (CH=CH) slightly was shifted to 5.67 ppm due to the coordination to a metal center. Similarly, the methylene ($-CH_2$) protons, which are adjacent to the carbonyl (-C=O) group appears at 1.60 ppm and β-methylene protons shifted to 2.34 ppm. The NMR spectra of purified (hexane washings) QDs displayed no residue that would otherwise appear at 0.85 and 1.23 ppm[19]. The broadening of the NMR peaks in oleate@ZnO QDs is due to the ionic character of the zinc-carbonyl bonding and poor solubility, when compared to the organic ligand and metal organic zinc oleate. Especially α and β protons, which are adjacent to the carbonyl groups, are influenced by the inhomogeneous nature of the local chemical environment that arises from the electron abundant surface of the ZnO QDs and different mode of bonding possible on the particle surface.

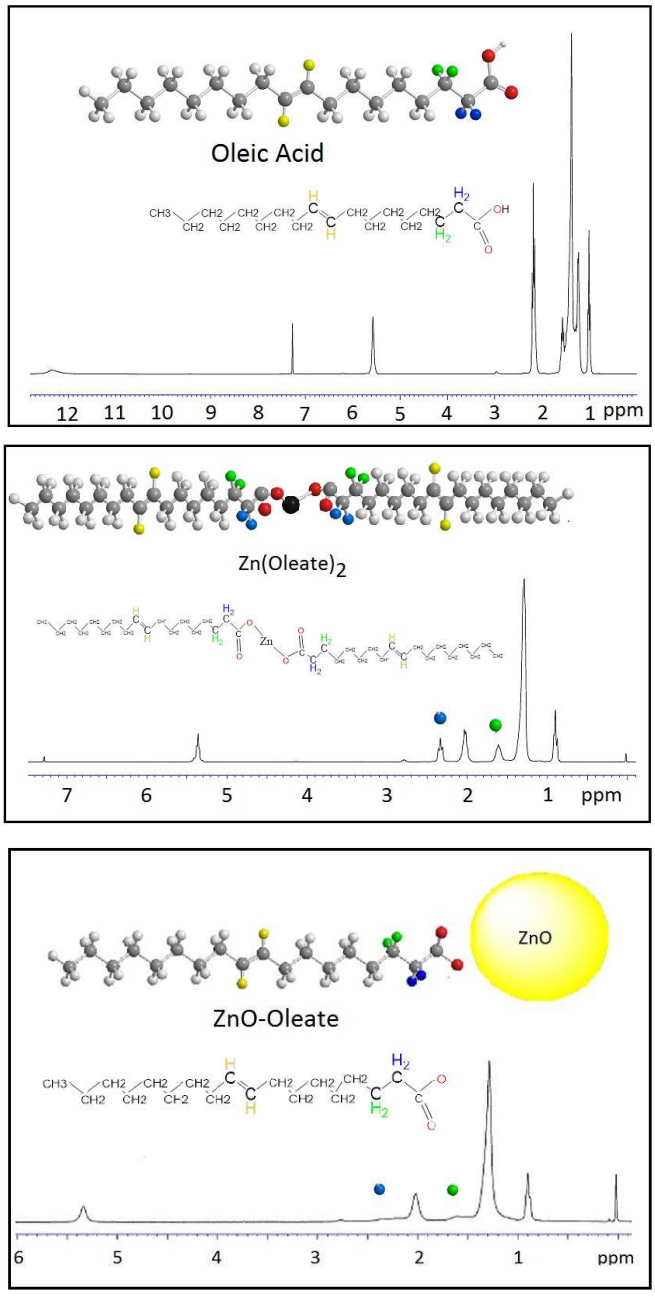

Figure 4: NMR investigation of oleate groups on the ZnO QD's

Consequently, the α-methylene protons ($-CH_2$) which are adjacent to the carbonyl (-C=O) group and β-methylene protons ($-CH_2$) almost disappeared due to local inhomogeneities and restricted motion of the protons[19] which is a clear evidence of oleate modification for ZnO QDs. The surface coverage by oleate groups was confirmed by FT-IR and thermo-gravimetry analysis (Supporting Figure 5).

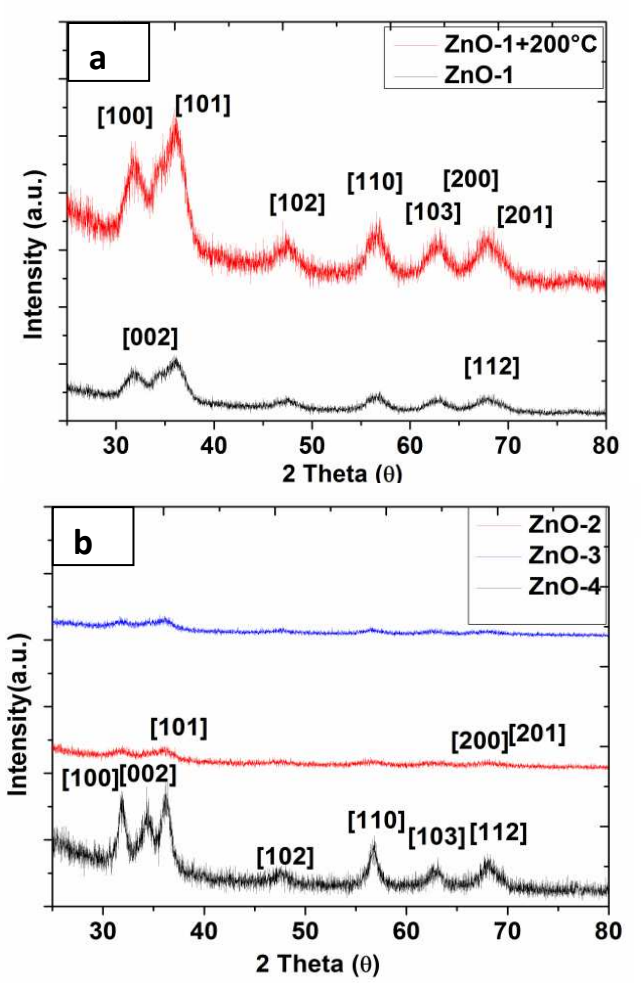

Figure 5: XRD analysis of a) ZnO-1(black) with ZnO-1+200° 3h (red) b) ZnO-2 (red), ZnO-3(blue) and ZnO-4(black)

The TEM analysis of samples after controlled calcination treatment (200°C, 2 hours) removed the oleate shell from the and ZnO core. Compared to the sol-gel synthesis (ZnO-4), the swift synthesis with minimum required synthesis duration and lower temperatures offer ZnO QDs that are well-shielded by in-situ generated oleate ligands. The driving force of the reaction is the higher basic character of hydroxo or alkoxo groups used for the activation of zinc oleate. The quantum dots after synthesis and purification steps were found to be stable for more than several months in EtOH or $CHCl_3$ with no evident changes in the spectral position of the visible emission size of the ZnO QDs. Peak broadening in the X-ray diffractograms (Figure 5) indicated very small grain size of the ZnO QDs, while sharpening of peaks was observed in samples heat-treated at 200°C as confirmed by XRD results and TEM images of the samples before and after heat treatment. Peak broadening in XRD spectra of the QD's is attributed to the very small grain size of the ZnO QD's.

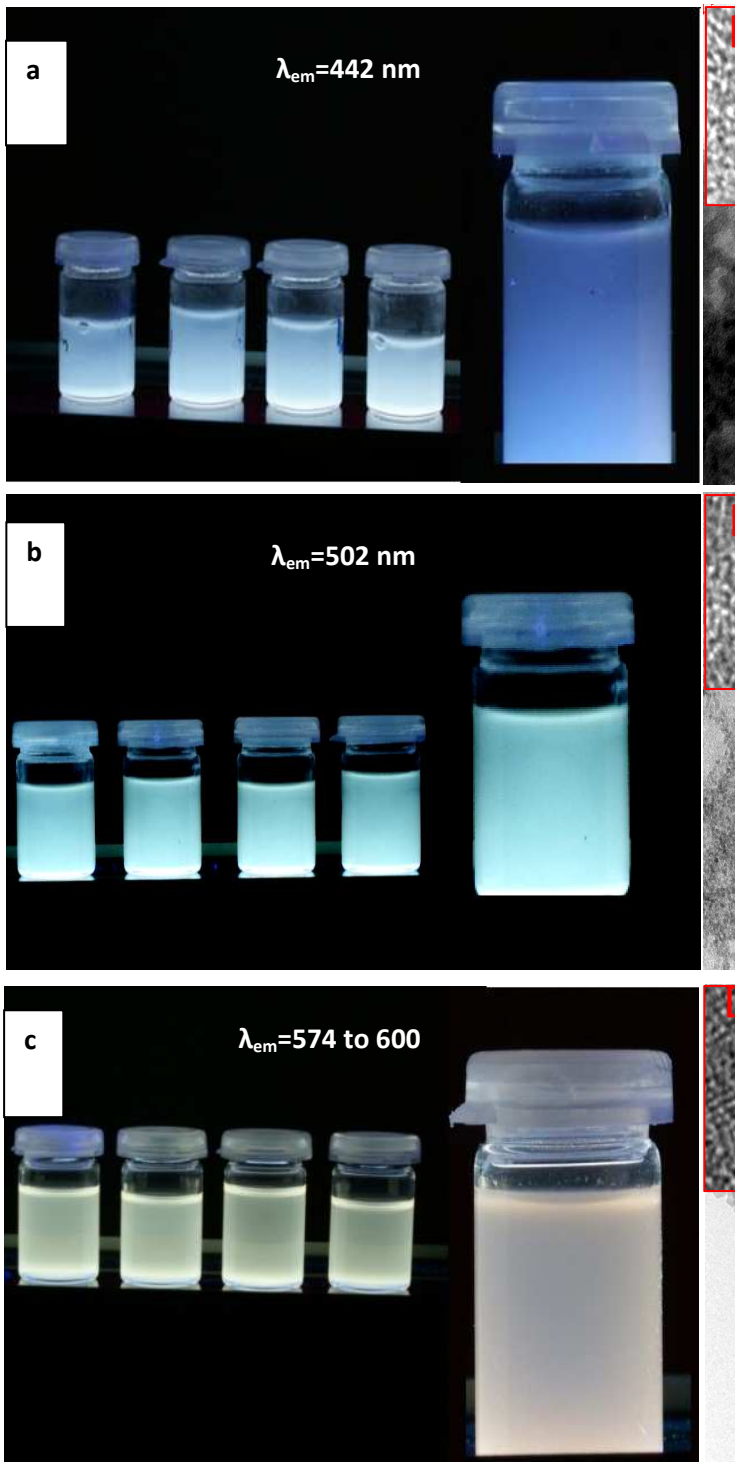

Figure 6: Visible emission of ZnO QDs with corresponding TEM spacing=0,26 nm, inset bars 2nm) a) ZnO-2, b) ZnO-3 and c) ZnO-

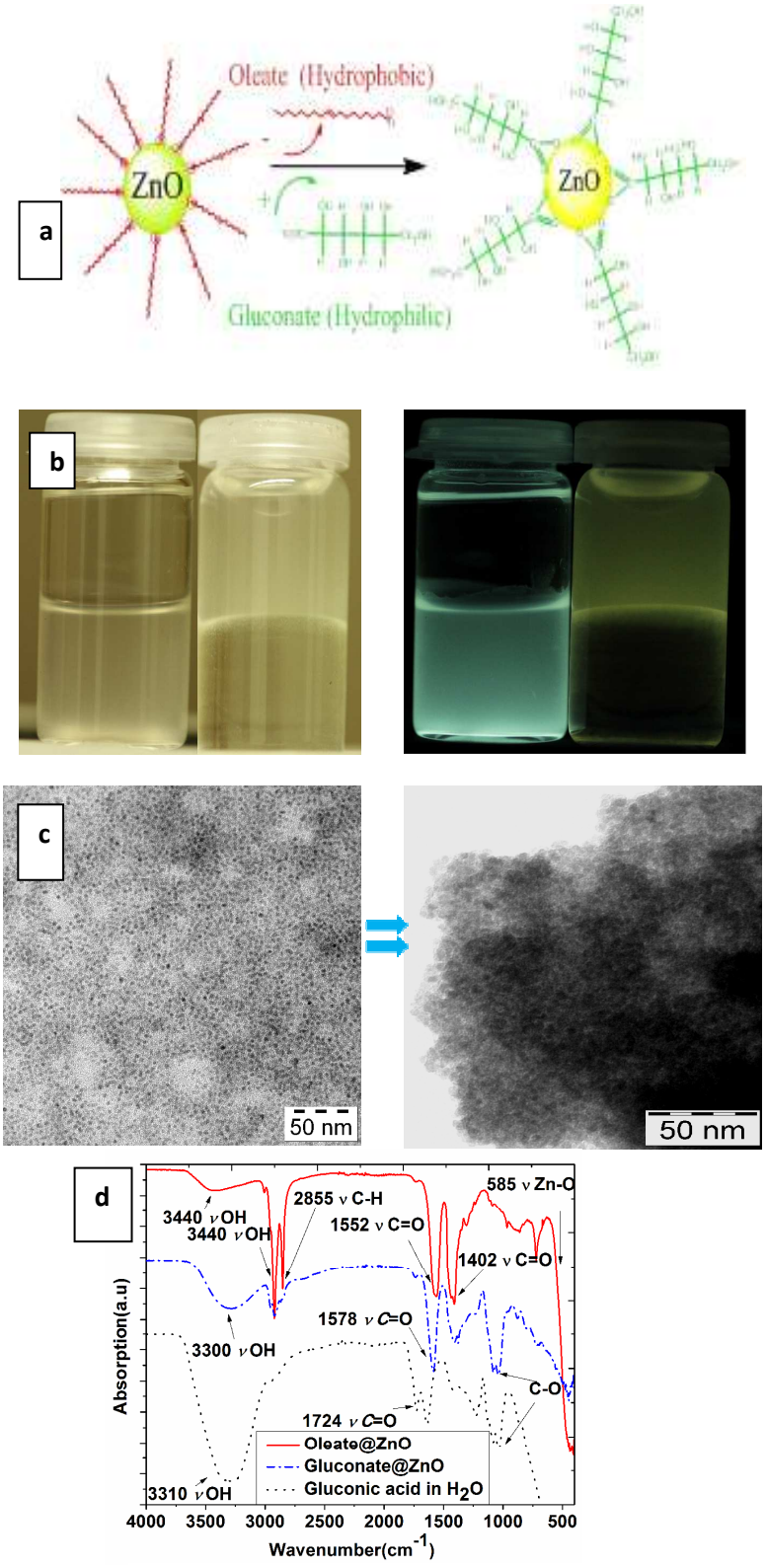

Figure 7: a) Phase transfer of the oleate@ZnO QDs with gluconic acid b) emission of phase-transferred QDs under UV illumination (λmax, 354 nm) c) TEM images before and after phase transfer with gluconic acid d) FT-IR confirmation of the ligand transfer on ZnO surface.

In the case of oleate@ZnO QDs, TEM investigation after the heat treatment depicted the spherical morphology with a predominant narrow size distribution. For the statistical size distribution, quantum dot sizes were numerically determined and plotted versus their frequency (Supporting Figure 8). The observed sizes are in agreement with the value obtained from the broadening of the XRD peak analysis by the Scherrer formula (4-5 nm for ZnO-1 and 5-6 nm for ZnO-4). It was difficult to calculate average grain size in ZnO-2 and ZnO-3 due to low diffraction intensities (Figure 5). Figure 6, shows HR-TEM pictures (insets) and suspension of Oleate@ZnO QD's in which visible light emission upon UV excitation exhibited clear transition from blue to yellow. Upon increasing the LiOH:Zn ratio (1:2 for ZnO-3) at the same temperature (55°C), the spectral position of the visible emission band became higher (λ_{max}= 502 nm) and slightly broader. ZnO QD particle sizes are practically bigger than those estimated by extrapolation of UV-Visible absorption spectra.

Absence of the hexane, alcohol, OH- or water in the final material is vitally important for stability of QDs during storage since their presence induces agglomeration due to hydrogen-bonding ultimately causing spontaneous growth manifested in the shift in the visible emission band. The amount of oleate groups onto the QDs could be deduced from the thermogravimetry (TGA) analysis (Supporting Figure 5). As a general feature, the samples ZnO-1, ZnO-2, and ZnO-3 showed both physically and chemically adsorbed ligands, whereas in the case of ZnO-4 adsorption of water is probable verified by the IR analysis of the samples and the observed weight loss (8-9%) below 250 °C. The decomposition of chemically bonded acetate groups was observed around 435 °C (weight loss 8%). A comparative analysis of the TG data showed two weight-loss and temperature regimes corresponding to removal of adsorbed and chemically grafted oleate groups (Supporting Figure 5).
In the case of oleate-coated ZnO QDs, oleate ligands attached to the surface were identifiable by asymmetric and symmetric carbonyl stretches of the carboxylic groups at 1564 and 1405 cm^{-1} that are different from the vibrational frequencies of the molecular precursor (Supporting figure 5). A shift in the position of carbonyl stretches (υ C=O) in FT-IR spectra is attributed to a change in the dipole moment of the carbonyl group, when ligand binds to metal or metal oxide surface with high electron density causing a shift to higher wave numbers. The samples undergoing ligand-exchange reactions with gluconic acid in water (50:50; v/v), peaks due to water appeared at 1630 cm^{-1} and in the range of 3200-3400 cm-1 (υ OH) together with the hydroxyl groups of the gluconic acid backbone. Carbonyl stretching (υ C=O) of the acidic function was observed at 1724 cm-1, which significantly shifted after the phase transfer reaction to exhibit asymmetric stretching to 1578 cm^{-1} and symmetric stretching to 1404 cm^{-1}. The relatively small peak at 1027 cm^{-1} that was observed at 1050 cm^{-1} before the phase transfer reaction can be attributed to heteroatomic stretching (C-O) of the substituted ligand. The position of Zn-O band (520 cm-1) remained unchanged. These observations are in good agreement with the 1H NMR data of the Gluconate@ZnO QDs (Supporting Figure 6).
Strikingly, the suspensions of ZnO QDs showed visible emissions of same intensity even after several months (Supporting Figure 7). In addition, the facile phase transfer reaction enabled the transfer of ZnO QDs from non-polar (for example CCl_4) to the aqueous phase (Figure 7). The driving force for the ligand-exchange reaction is the removal of oleate group (pKa of oleic acid: 9.85)[20] with a ligand of lower pKa value acid (pKa of gluconic acid: 3.7)[21]. The general applicability of the phase-transfer phenomena was demonstrated for mandelic acid (pKa: 3.41)22 and poly-hydroxy carboxylic acids like citric acid (pKa1:2.8, pKa2:4.1 and pKa3:5.3)[23] and confirmed by FT-IR spectral data (not shown) recorded before and after the phase-transfer reactions. Due to its hydrophilic nature, gluconic acid coating caused an aggregation of ZnO QDs as clearly observed in the TEM images (Figure 7). After the phase transfer step, the spectral position of the visible emission (542 nm) of oleate-capped ZnO

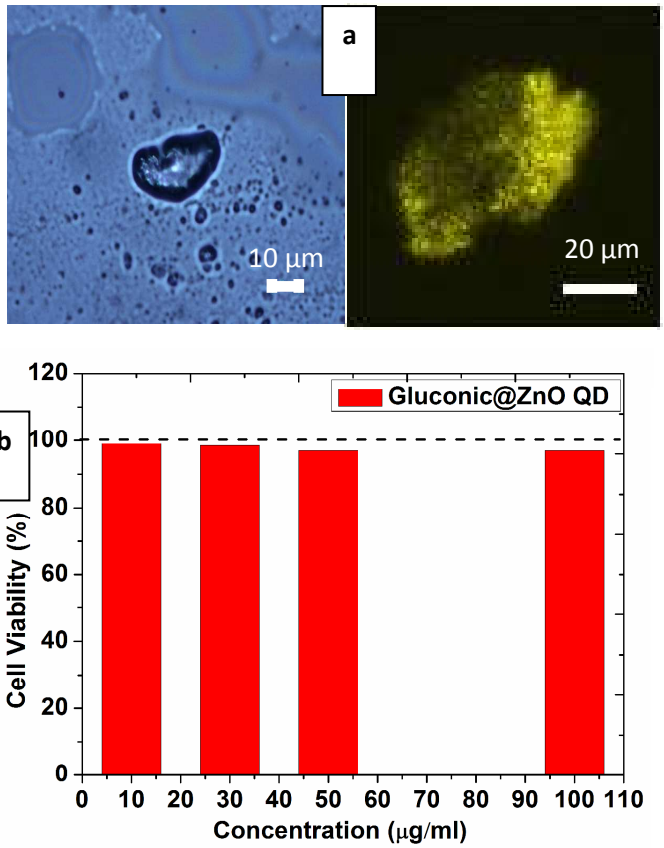

Figure 8: a) Confocal images of the HEK cells after 2h incubation with Gluconate@ZnO QD's b) MTT test for the cell viability during 4 h with different dosing

QDs showed a slight bathochromic shift (547 nm) for the gluconate@ZnO QD's. The high intensity of the visible emission can possibly result from a decrease in the oxygen deficiencies on ZnO surface due to multiple chelating sites (hydroxyl groups) available in the gluconic acid molecules.

The objective of preparing ZnO QDs easily dispersible in aqueous system was to assess their cytotoxic properties and potential for cell labeling (Figure 8a) applications.[24-29] Previous studies already showed that ZnO nanoparticles show dose-dependent cellular toxicity.[30-32] After the phase transfer process, aqueous solution of gluconate@ZnO QD's were used in labeling of Human Embryonic Kidney 293 (HEK 293) cells. Cytotoxicity level of the gluconate@ZnO QD's on HEK 293 cells was determined by the MTT assay as previously described. To examine the concentration effects, different amountd of gluconate@ZnO QDs (10μg/ml, 30 μg/ml, 50 μg/ml, 100 μg/ml) were added into titer wells and incubated for 4h at 37°C into 20μl MTT. The cell studies revealed a low viability loss (3-5 %) during 4 hours as plotted in Figure 8b. The confocal microscopy images of the prepared HEK cells on glass slides under suitable excitations confirmed the cellular uptake and efficient visible emission.

Conclusions

In summary, a facile method for the preparation of the highly luminescent, hydrophobic Oleate@ZnO QDs with highly efficient visible emission and ultrastable storage behavior even after several months storing is reported. QD's showed. Visible emission properties were controlled by chelation of various surface ligands to produce blue and green emitting QDs. In addition, the successful demonstration of phase-transfer reactions delivered water soluble QDs that can have important implications in nanoelectronics, printable TCOs and cell labeling applications.

Acknowledgements

We gratefully acknowledge the University of Cologne and Nanommune Project (EC-FP7-NANOMMUNE-Grant Agreement No. 214281) for the financial support, Dr. Hao Shen for the HR-TEM measurements and discussions, Muhammed Sajid Hussain for the Confocal Microscopy measurements, Karim Arroub for the MTT test and Dr. Wieland Tyrra for the fruitful NMR discussions.

Notes and references

[a] Institute of Inorganic Chemistry, University of Cologne, D-50939 Cologne, Germany, Fax: +49 221 470 4899; Tel: +49 221 470 4107; Correspondence: sanjay.mathur@uni-koeln.de

[b] Institute of Physical Chemistry, University of Cologne, D-50939 Cologne, Germany

Electronic Supplementary Information (ESI) available: Additional TEM investigations, UV-Vis and photoluminescence results, thermal analysis, agglomeration behavior, molecular FT-IR analysis of the precursors, stability details and quantum dot size distribution are available as a Supporting Info. See DOI: 10.1039/b000000x/

References

[1] a) A. P. Alivisatos, Science, 1996, 271, 933; b) M. H.Huang, S. Mao, H. Feick, H. Q.Yan, Y. Y.Wu, H. E. Kind, R. Russo and P. D. Yang, Science 2001, 292, 1897 c) C. H. Liu, J. A. Zapien, Y. Yao, X. M. Meng, C. S. Lee, S. S. Fan, Y. Lifshitz and S. T. Lee,Adv. Mater., 2003, 15, 838 d) L.E. Greene, B.D. Yuhas, M. Law, D. Zitoun and P. Yang, Inorg. Chem., 2006, 45, 7535.

[2] a) Z.L.Wang, J. Phys.Condens.Matter, 2004,16,829; b) G. Yi, C.Wang and W.I. Park, Semicond. Sci. Technol., 2005,20,22 c) L. Schmidt-Mende and J.L. MacManus-Driscoll,Materials Today, 2007,10,40 d) A.B. Djurisic, X. Chen, Y. H. Leung, and A.M. Ching Ng, J. Mater. Chem., 2012, 22,6526 e) J.A. Anta, E.Guillén, R.Tena-Zaera, J. Phys. Chem. C, 2012,116,11413.

[3] a) A. B. Djurisic, Y. H. Leung, K.H. Tam, Y. F. Hsu; L. Ding, W.K. Ge, Y.C. Zhong, K.S. Wong, W.K. Chan, H.L. Tam, K.W. Cheah, W.M. Kwok and D.L. Phillips,Nanotechnology, 2007,18,95702; b) A. B. Djurisic, Y. H. Leung, K. H. Tam, L. Ding, W. K. Ge, H.Y. Chen and S. Gwo, App.Phys. Lett., 2006, 88, 103107; c) A.B. Djurisic and Y. H. Leung, Small, 2006, 2, 944.

[4] a) X.L. Chen, C.S. Xu, Y.X. Liu, S.L. Liang, H.Q. Qiao, H.T. Xu, Y.H. Ning and Y.C. Liu, J. Nanosci. Nanotechnol., 2011,11,9415 b) L. Spanhel and M.A.Anderson, J. Am. Chem. Soc., 1991,113,2826 c) S. Tachikawa, A. Noguchi, T. Tsuge, M. Hara, O. Odawara and H. Wada,Materials, 2011,4,1132.

[5] a) G.Yi, C. Wang, W.I. Park, Semicond. Sci. Technol., 2005,20,22 b) Y. Zhong, A.B. Djurišić, Y.F. Hsu, K.S. Wong, G. Brauer; C.C. Ling and W.K. Chan,J. Phys. Chem. C, 2008,112,1628 c) S. Wu, Q. Tai and F. Yan, J. Phys. Chem. C, 2010,114,6197 d) S.Y. Bae, H.W. Seo, H.C. Choi and J. Park, J. Park, J. Phys. Chem. B, 2004,108,12318 e) V.G. Pol J. M. Calderon-Moreno and P. Thiyagarajan,Langmuir, 2008,24,13640 f) P. A. Rodnyi and I. V. Khodyuk, Optics and Spectroscopy, 2011,111, 776.

[6] a) L. Qu and X.Peng, J. Am. Chem. Soc., 2002,124,2049 b) G.A. Beane, A.J. Morfa, A.M. Funston and P. Mulvaney, J. Phys. Chem. C, 2012, 116,3305.

[7] a) J. Cui, J. Phys. Chem. C, 2008, 112,10385 b) X. Tang, E.S.G. Choo, L. Li, J. Ding and J. Xue, Langmuir, 2009, 25,5271; c) H. Zeng, G. Duan, Y. Li, S. Yang, X. Xu, W. Cai, Adv. Funct. Mat., 2010, 20,(4) 561.

[8] Djurišić A.B.; Ng A.M.C.; Chen X.Y.; ZnO nanostructures for optoelectronics: Material properties and device applications Progress in Quantum Electronics 2010, 34, 191.

[9] a) A. van Dijken, E. A. Meulenkamp, D. Vanmaekelbergh and A. J. Meijerink, Phys. Chem. B, 2000,104,1715 b) A. van Dijken, E. A. Meulenkamp, D. Vanmaekelbergh and A. J. Meijerink, J. Phys. Chem. B, 2000,104,4355 c) A. van Dijken, E. A. Meulenkamp, D. Vanmaekelbergh and A. J. Meijerink,J.of Luminescence, 2000,87–89,454 d) A. van Dijken, J. Makkinje and A. Meijerink, J. of Luminescence, 2001,92,323 e) A. van Dijken, E. A. Meulenkamp, D.

Vanmaekelbergh and A. J. Meijerink, J.of Luminescence, 2000, 90,123.
[10] a) R.S. Devan, R.A. Patil, J. Lin and Y.R. Ma, Adv. Funct. Mat., 2012,22,3326 b) Q. X. Zhao, P. Klason, M. Willander, H. M. Zhong, W. Lu and J. H. Yang, Appl. Phys. Lett., 2005,87, 211912.
[11] a) C. Klingshirn, Phys. Stat. Sol., 2007, 244, 3027 b) S. Sakohara, L.D. Tickanen and M. A. Anderson, J. Phys. Chem., 1992, 96,11086
[12] Y. Fu, X. Du, S.A. Kulinich, J. Qiu, W. Qin, R. Li, J. Sun and J. Liu,J. Am. Chem. Soc., 2007,129,16029.
[13] M. Abdullah, S. Shibatomo and K. Okuyama,Opt. Mater., 2004,26,95.
[14] H.M. Xiong, Z.D. Wang and Y.Y. Xia, Adv.Mater., 2006,18,748.
[15] Meulenkamp E. A. Synthesis and Growth of ZnO Nanoparticles J. Phys. Chem. B, 1998,102, 5566
[16] a) L. Zhang, L. Yin, C. Wang, N. Lun, Y. Qi and D. Xiang, J. Phys. Chem. C, 2010, 114, 9651 b) H.M. Xiong, J. Mater. Chem., 2010, 20, 4251 c) S. Sakohara, M. Ishida and M.A. Anderson, J. Phys. Chem. B, 1998, 102,10169.
[17] a) R. Viswanatha, H. Amenitsch, D. D. Sarma, J. Am. Chem. Soc.2007, 129 (14), 4470−4475 b) A. Dakhlaoui, M. Jendoubi, L.S. Smiri, A. Kanaev, N. Jouini J. Cryst. Growth 2009, 311 (16), 3989−3996 c) P. K. Santra, S. Mukherjee, D. D. Sarma, J. Phys. Chem. C 2010,114 (50), 22113−22118 d) K. D. Kim, D. W. Choi, Y. H. Chou, H. T. Kim, Colloids Surf.,A 2007, 311 (1−3), 170−173
[18] a) H. M. Xiong, R. Z. Ma, S. F. Wang, Y. Y. Xia, J. Mater. Chem.2011, 21 (9), 3178−3182, b) S.Li, Z. Sun, R. Li, M. Dong, L. Zhang, W. Qi, X. Zhang, H. Wang, Sci Rep. 2015; 5: 8475 c) H.-M. Xiong, D.G. Shchukin, H. Möhwald, Y. Xu, Y.-Y. Xia, Angew. Chem. Int. Ed., 2009, 48: 2727–2731 d) A. Glaria, M.L. Kahn, T. Cardinal, F. Senoc, V. Jubera, B. Chaudret, New J. Chem., 2008, 32, 662–669 e)R. Moussodia, L. Balan, R. Schneider, New J. Chem., 2008, **32**, 1388-1393 f) D. P. Liu, G. D. Li, Y. Su, J. S. Chen Angew. Chem. Int. Ed. 45, 7370–7373 (2006).
[19] a) O. Kohlmann, W. E. Steinmetz, X. A. Mao, W. P. Wuelfing, A. C. Templeton, R. W. Murray; C. S.Johnson, J. Phys. Chem. B, 2001, 105, 8801 b) A. Hassinen, I. Moreels, de M. Donega C., J.C. Martins and Z. Hens,J. Phys. Chem. Lett. 2010, 1, 2577
[20] J.R. Kanicky and D.O. Shah, J. of Coll.Int. Sci., 2002, 256, 201
[21] S. Ramachandran, Food Technol. Biotechnol., 2006, 44,185
[22] MB. Taylor, Cosmetic Dermatology, 1999, 21, 26-28.
[23] P.C. Hidber, T.J. Graule and L.J. Gauckler, J Am. Ceram. Soc., 1996,79, 1857
[24] T. Buerki-Thurnherr, L. Xiao, L. Diener, O.Arslan, C. Hirsch, X. Maeder-Althaus, K. Grieder, B. Wampfler, S. Mathur, P. Wick and Krug, H. Nanotoxicology, 2012,7, 402
[25] S. Tuomela, R. Autio, T. Bürki-Thurnherr, O. Arslan, A. Kunzmann, B. Andersson-Willman, P. Wick, S. Mathur, A. Scheynius, H. Krug, B. Fadeel and R. Lahesmaa, PLoS ONE, 2013,8,e68415
[26] O. Arslan, A.P. Singh, L. Belkoura, S. Mathur,J.of Materials Research, 2013, 28, 1947
[27] H. Shi, W. Li, L. Su, Y. Liu, H. Xiao and S. Fu,Chem. Commun., 2011, 47, 11921
[28] M. Eita, R. El Sayed and M. Muhammed,J. Coll.Int. Sci., 2012, 387, 135
[29] F. Muhammad, M. Guo, Y. Guo, W. Qi, F. Qu, F. Sun, H. Zhao and J.Gu,Mater. Chem., 2011, 21, 13406
[30] a) H. Zhang, H. Xiong, Q. Ren, Y. Xia and J. Kong, J. Mater. Chem., 2012, 22, 13159 b) R. Moussodia, L. Balan, C. Merlin, C. Mustin and R. Schneider,J. Mater. Chem., 2010,20, 1147
[31] Y. Zhang, X. Wang, Y. Liu, S. Song and D. Liu,J. Mater. Chem., 2012,22, 11971
[32] A) N. S. Norberg and D. R. Gamelin, J. Phys. Chem. B, 2005, 109, 20810 b) S.T. Teklemichael and M.D. McCluskey,J. Phys. Chem. C, 2012, 116, 17248

Swift method was developed for highly luminescent, monodispersed, hydrophobic Oleate@ZnO QD by sol-gel providing ultralong stability and possible scaling up opportunity.

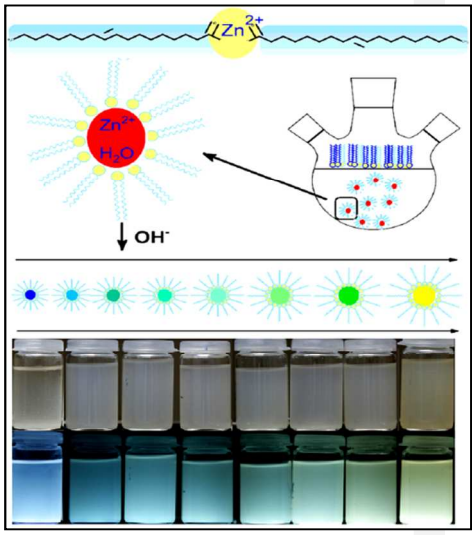

Osman Arslan,[a] Lhoussaine Belkoura[b] and Sanjay Mathur[a],*……

Swift Synthesis, Functionalization and Phase-transfer Studies of Ultrastable, Visible Light Emitting Oleate@ZnO Quantum Dots

Keywords: Ultrastable ZnO QD's / phase transfer / Oleate capping/ cell labeling

TOC

Swift Synthesis, Functionalization and Phase-transfer Studies of Ultrastable, Visible Light Emitting Oleate@ZnO Quantum Dots